

Raman measurements of the vibrational properties of H₂ as a guest molecule in dense helium, neon, argon, and deuterium systems up to 40 GPa

P. Loubeyre, R. LeToullec, and J. P. Pinceaux

Physique des Milieux Condensés, Université Paris VI, 4 place Jussieu, 75252 Paris, France

(Received 7 November 1991)

The vibron peak of the H₂ molecule diluted in helium, neon, argon, and deuterium host systems have been measured up to 40 GPa by Raman scattering. A blue shift of the vibron frequency is observed in all these systems. The line shape of the vibron peak is seen to be essentially due to inhomogeneous broadening. The experimental data allow a quantitative analysis of the various contributions to the vibron frequency shift: static shift, dynamical shift, and vibrational coupling. The strong differences between the vibron frequency shift of the H₂ molecule embedded in solid D₂ and in solid H₂ are seen to result essentially from the vibrational coupling contribution. The large negative vibrational constant associated with it could be an indication of the presence of the charge-transfer interaction, already important in this density range.

I. INTRODUCTION

An extensive literature covers the field of matrix-isolation spectroscopy, motivated by an understanding of elementary molecular processes in condensed matter and by interesting issues in astrophysics and physical chemistry.¹ Progress in the field has followed mainly the refinement of the techniques of spectroscopy, promoting studies in the time and frequency domain, and a great deal of information about dynamical processes has already been obtained. Another branch of research in this field has been to extend the measurements at high pressure. The Raman and infrared measurements of spectral shifts are considered to allow an effective direct test of theoretical intra- and intermolecular potentials, but they were, until very recently, limited to below 1 GPa.² The vibron frequency of H₂ isolated in a Ne matrix was recently reported to increase strongly with pressure,³ whereas the vibron frequency of H₂ in its solid has been found to present a maximum around 30 GPa.⁴ So, going to higher pressures, other questions arise such as the validity of the molecular approach or the interrelationship between intra- and interelectronic densities.

The present article reports measurements above 1 GPa of the vibrational properties of a H₂ molecule isolated in different matrices, here He, Ne, Ar and D₂, mainly at room temperature. A membrane diamond anvil cell (MDAC) was used to generate pressures above 40 GPa. A strong blue shift of the vibron mode with pressure has been observed, surprisingly even for H₂ isolated in D₂ solid. This work is organized as follows: The experimental conditions will be described in Sec. II; the measurements of the frequency and the line shape of the vibron of H₂ guest molecules in dense He, Ne, Ar, and D₂ systems will be presented, respectively, in Sec. III for the liquid phase and Sec. IV for the solid phase. In Sec. V, the discussion of the data will emphasize two results: first, the limitation under pressure of the description of the properties of the isolated H₂ molecule within the molecular

approach, that is based on the knowledge of the intra- and intermolecular potentials; second, the existence of a strong vibrational coupling between H₂ molecules, with a negative vibrational constant which helps to understand the special features of the vibrational properties of dense solid H₂.

II. EXPERIMENTAL METHODS

The majority of previous measurements on matrix-isolated molecules at high pressures were done in a gas cell wherein the pressures were limited to below 1 GPa.⁵ Very high pressures are now routinely generated on pure molecular systems with the use of the diamond anvil cell.⁶ The diamond anvil cell is a mechanical device to push two opposed diamond anvils so as to compress a metallic shim. The sample chamber is constituted by a cylindrical hole drilled in the shim sealed by the two anvils, which constitute excellent optical windows. Although pressures of the order of 40 GPa can now be routinely obtained on molecular systems, the application of this technique to matrix spectroscopy has been delayed until now for essentially the two following reasons: It was necessary to study the properties of the undoped crystals (rare gases and H₂) first; second, the very small volume of the sample chamber gives weak spectroscopic signals on these diluted systems (as a matter of fact, the rotational line could not be measured in the present Raman study mainly because their spectra were hidden by the fluorescence of the diamonds).

The present experiments have been performed in a membrane DAC; its design and loading system have been described elsewhere.⁷ High-purity (99.9%) commercial gases were used; the gaseous mixtures were made under a pressure of 10 MPa at room temperature and their concentrations were estimated by the ratio of partial pressures corrected with the first virial coefficients. The mixture was then pressurized to 100 MPa for loading the cell at room temperature. Beryllium-Copper gaskets were

used to prevent any diffusion of H_2 in the gasket during the experiment. The sample chamber was typically 150 μm in diameter and 20 μm thick at 40 GPa. The pressure was measured with the ruby fluorescence technique and the quasihydrostatic calibration scale.⁸ Raman spectra in matrices were obtained with an Ar^+ laser excitation at 488 nm, a triple T800 Coderg spectrometer, and photon-counting electronics. Relatively high power (300 mW) was used with no measurable heating effects and the spectrometer slit width was opened to 300 μm giving an experimental resolution of 3 cm^{-1} . The experiments were performed at room temperature and extended once to 113 K in a cryostat for H_2 in a Ne matrix. For pure H_2 , lower power (100 mW) could be used and the spectrometer slit width was closed to 100 μm , improving the experimental resolution to 1 cm^{-1} .

Before presenting the data in the next section, we should first define at which concentrations the H_2 molecule can be considered as isolated in the rare-gas matrices. In Fig. 1, the Raman measurements of the $Q_1(1)$ vibron mode frequency of H_2 in H_2 -Ne fluid mixtures of various H_2 concentrations, ranging from 10 to 0.5 mol %, are compared. It is seen that the data do not change anymore with concentration for H_2 concentrations smaller than 2 mol %. That is when the low concentration limit is reached. All our experiments were performed within this limit. For H_2 in D_2 , slightly higher H_2 concentrations (4 mol %) were used so as to compensate for the fraction (roughly 50%) of H_2 molecules which react with a D_2 molecule to form HD molecules.

It should also be noted that, under pressure, there is no distinction between the vibron modes of ortho- H_2 and para- H_2 molecules because of motional narrowing.⁹ Essentially, because of the increased rotationally inelastic collision frequency with pressure at room temperature, the distinction between the different vibration lines corresponding to different J rotational states is lost. Thus, the

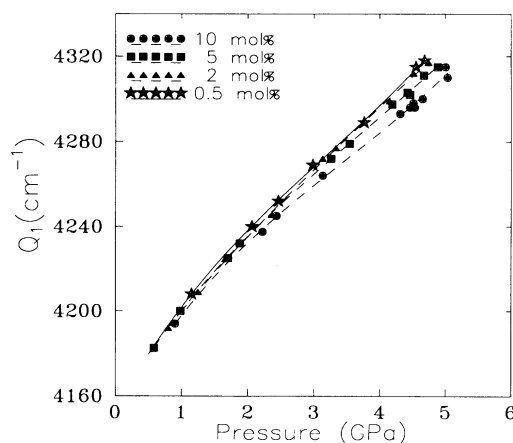


FIG. 1. Comparison of the Raman frequency shift with pressure of the $Q_1(1)$ vibron mode of H_2 molecules embedded in different H_2 -Ne fluid mixtures at low H_2 concentrations. The circles represent the data for a H_2 concentration of 10 mol %; the squares, the ones for 5 mol %; the triangles, the ones for 2 mol %; and the stars, the ones for 0.5 mol %.

molecule takes on a vibrational frequency corresponding to the rotation-vibration coupling for some mean value of the rotational quantum number $\langle J \rangle$. In normal H_2 at room temperature, there is only one vibrational peak $Q_1(\langle J \rangle=1)$, with a half-width of 15 cm^{-1} in the fluid phase and of 6 cm^{-1} in the solid phase.⁴

III. FLUID PHASE

Typical Raman spectra for 2-mol % H_2 molecules in He, Ne, Ar, and D_2 fluids, near their crystallization, are compared to the one of pure H_2 in Fig. 2. The signal-to-noise ratio is of the order of 4 and the maxima of the peaks could be pointed with an accuracy of $\pm 1 \text{ cm}^{-1}$. The line shapes are slightly asymmetrical with a low-frequency tail and their half-width, around 25 cm^{-1} , is greater than the one in pure fluid H_2 . In our previous study on the vibrational properties of a H_2 molecule in homogeneous H_2 -He fluid mixtures,¹⁰ the line shape of the vibron mode was shown qualitatively to result mainly from inhomogeneous broadening. This explanation is also valid here in the low H_2 concentration limit case: A fluctuation of local concentration will change the vibron frequency only when it falls outside the low concentration limit domain, that is, for H_2 local concentrations greater than 2 mol %; this produces a vibron frequency decrease that builds up the low-frequency tail. This will be analyzed in more detail below for the solid phase.

The $Q_1(1)$ vibron frequency shift versus pressure in these various fluid systems is compared in Fig. 3. All the experiments were started above 0.3 GPa since, below, variations of concentration might occur during the loading procedure. The data are fitted by third-order polynomials, the coefficients of which are reported in Table I. This mathematical form certainly has no physical significance but it allows a concise presentation of the experimental data without any loss of information since the deviations between the fits and the data are smaller than the error bars. The measurements were redone in pure fluid H_2 and they agree with previous determinations.⁴

In room-temperature experiments of H_2 in rare-gas fluids up to 700 amagat, a frequency red shift of the $Q_1(J)$ lines was reported.¹¹ These experiments were complemented by theoretical works which could reproduce both the frequency shift and width in the framework of binary collision approximation.¹² As seen in Fig. 3, upon further increasing the density, a frequency shift inversion is passed and for pressures above 0.3 GPa the shift is strongly blue shifted. A reasonable explanation is that the guest-host interaction has moved from its attractive region to its repulsive one. Therefore, the present data could be used to test and to refine the repulsive wall of the interactions between H_2 and rare-gas atoms (He, Ne, Ar). More particularly, these data constitute one of the few experimental properties directly sensitive to the dependence of the intermolecular potential on the H_2 diatomic bond length. Such an analysis is beyond the scope of the present article but still a qualitative remark can be made: The H_2 -rare-gas potentials seem to differ strongly from their estimate with Berthelot-Lorentz combination rules.¹³ For proof, the $Q_1(1)$ vibron frequency of H_2 in a

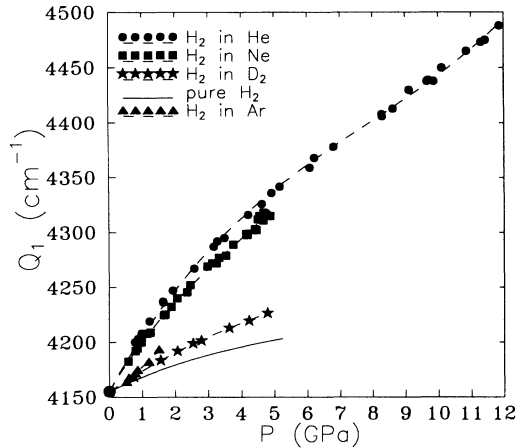


FIG. 3. Change vs pressure at room temperature of the Raman frequency of the $Q_1(1)$ vibron model of the H_2 molecule isolated in various fluids. The circles represent the data in the He fluid; the squares, the data in the neon fluid; the stars, the data in the D_2 fluid; and the triangles, the data in the Ar fluid. The solid line is the third-order polynomial fit to the measurements in pure fluid H_2 and the dashed lines, the fits of the data in the other fluids. The coefficients of these fits are given in Table I.

overlap forces for the vibrational coupling will be addressed.

IV. SOLID PHASE

The extension of the above-described fluid measurements in the solid phase was complicated both by the lower solubility of H_2 in the solid than in the fluid phase of rare gases and also by aggregation processes. Suffice it to say here that the solubility of H_2 in solid He is very small, less than 0.3 mol %, and most of it under clusters resulting from a segregation process; consequently, the vibrational spectra of the monomer H_2 in a He matrix was too weak to be detected. The solubility of H_2 in solid Ar is slightly greater, of the order of 0.5 mol %, and the segregation process smaller than in He; as seen below, the vibrational spectra of monomer H_2 in an Ar matrix could be measured. Finally, the solubility of H_2 in solid Ne is very large above crystallization since up to at least 10 mol % of H_2 can be mixed with Ne in a homogeneous solid. With pressure, this solubility decreases and tends to 5 mol % above 15 GPa. Also, no segregation occurs and the existence of clusters originates from the random

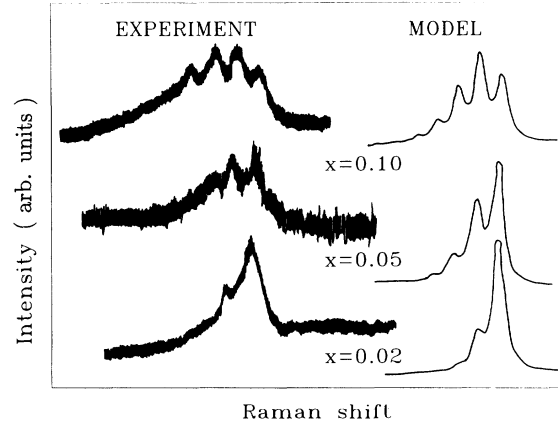


FIG. 4. Left: Experimental $Q_1(1)$ vibron spectra of the H_2 molecule embedded in homogeneous H_2 -Ne solid mixtures around 6 GPa at 296 K. Right: Calculated line shapes, as explained in the text in Sec. IV. All the spectra have the same scale in cm^{-1} . x is the H_2 concentration in mol %.

distribution of H_2 molecules on the substitution lattice sites of solid Ne.

In Fig. 4, the Raman lineshapes of the $Q_1(1)$ vibron mode of H_2 molecules embedded in homogeneous H_2 -Ne solids are compared at pressures around 6 GPa and for H_2 concentrations of, respectively, 10, 5, and 2 mol %. The Q_1 branch is constituted of resolved components equally spaced. The maxima of these structures have fixed frequencies at a given pressure and changes in the shape of the band appear to be due merely to changes in the relative intensities of the maxima. These line shapes can be accounted for under the following assumptions: First, a random distribution of H_2 molecules on the substitutional sites of the Ne lattice; secondly, a shift of the vibron frequency of the H_2 molecule proportional to the number j of its nearest-neighbor Ne atoms; thirdly, a Lorentzian vibron peak of half-width γ independent of j . Then, at a given pressure P and for a molar concentration of Ne atoms, x , the line shape is given by the following formula:

$$I(\omega) = \sum_{j=0}^{12} \frac{12!}{j!(12-j)!} x^j (1-x)^{12-j} \frac{\gamma^2/4}{[\omega - \omega(j)]^2 + \gamma^2/4} \quad (1)$$

with

TABLE I. Coefficient of the third-order polynomial, $Q_1(cm^{-1}) = a_0 + a_1P + a_2P^2 + a_3P^3$ with P in GPa fits to the Raman measurements of the shift with pressure of the $Q_1(1)$ vibron frequency of the H_2 molecule isolated in various fluids: He, Ne, Ar, D_2 , and H_2 .

System	a_0	a_1	a_2	a_3
H_2 in He	4155.2	53.7322	-4.3529	0.1853
H_2 in Ne	4155.2	50.6948	-6.0959	0.5305
H_2 in Ar	4155.2	16.9893	5.9985	-0.3564
H_2 in D_2	4155.2	20.1806	-1.3268	0.0448
H_2 in H_2	4155.2	14.6284	-1.3441	0.0593

$$\omega(j) = \frac{\omega_m - \omega_{H_2}}{12} j + \omega_{H_2},$$

where ω_{H_2} and ω_m are, respectively, the $Q_1(1)$ vibron frequency of the H_2 molecule embedded in its solid and in a Ne matrix.

As seen in Fig. 4, the line shapes calculated with this model compare favorably with experiment. In the liquid phase, such structures of the $Q_1(1)$ branch are smeared out in a low-frequency tail for H_2 concentrations smaller than 5 mol %. This corroborates the fact that the line shape of the $Q_1(1)$ vibron mode of the diluted H_2 molecule is essentially due to inhomogeneous broadening. It is also clear why the low concentration limit has been found around 2 mol % since there the intensity of the monomeric peak largely overcomes the ones of the clusters of 2, 3, or 4 molecules.

In Fig. 5, the line shapes of H_2 in the Ne, Ar, and D_2 matrices are presented at their maximum pressure of investigation. The signal-to-noise ratio is, at worse, 2 and the peak maxima could be pointed with a resolution of $\pm 2 \text{ cm}^{-1}$. However, the extension of the present measurements at very high pressure will not be straightforward and will certainly require more spectroscopic

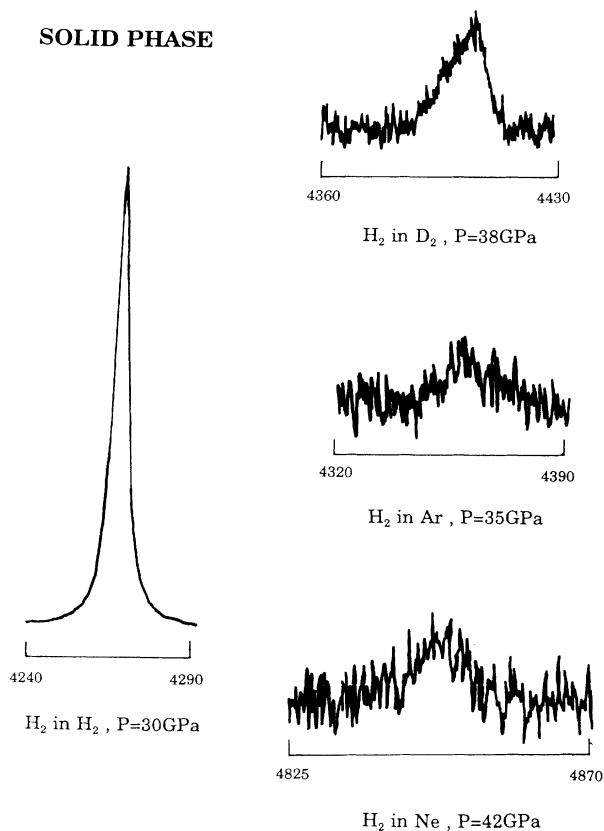


FIG. 5. Typical room-temperature Raman spectra of the $Q_1(1)$ vibron mode of the H_2 molecule isolated in different matrices, Ne, Ar, D_2 , and pure H_2 , at their maximum pressure of investigation. The instrumental resolution was 3 cm^{-1} , except for pure solid H_2 where it was improved to 1 cm^{-1} . The edges of the spectra are indicated in cm^{-1} .

efforts: Very high pressures are obtained at the expense of volume and a reduction of the volume of the sample by a factor 20 will be necessary in order to achieve pressures in the 100 GPa range. So, with the spectroscopic setup used in the present measurements, the signal would fall into the noise.

In Fig. 6, the evolutions with the pressure of the $Q_1(1)$ vibron frequency of H_2 molecules isolated in the Ne, Ar, and D_2 matrices are compared to the one in pure solid H_2 . Our measurements in solid H_2 are in very good agreement with previous determinations.⁴ In matrices, the $Q_1(1)$ vibron model exhibits a monotonic blue shift with pressure, quite strong in the case of the Ne matrix. The compressional trend is in agreement with theoretical predictions given either by quantum-mechanical calculations, such as the box model,¹⁷ or by the molecular approach.¹⁸ According to the box model, this monotonic increase of the frequency should continue up to very high pressure until ionization of the H_2 molecule.

As for the fluid case, the data were fitted by third-order polynomials with a concern of conciseness and usability for future comparison with theory. The coefficients of these fits are given in Table II.

The experimental discontinuity of the vibron shift at the crystallization of the host system is positive, $+3 \times 10^{-3}$ for Ne and $+10^{-4}$ for D_2 , but negative, -5×10^{-3} , for Ar. This is interesting experimental information for a sensitive test of binary intermolecular potentials. If the compressional efficiency of the fluid and solid host systems were the same, at crystallization the positive discontinuity would be directly related to the positive discontinuity of density. This is mostly the case for the D_2 host system where the discontinuity is seen to be small, but this has to be corrected by the fact that, in the solid phase, the H_2 molecule sits on substitutional

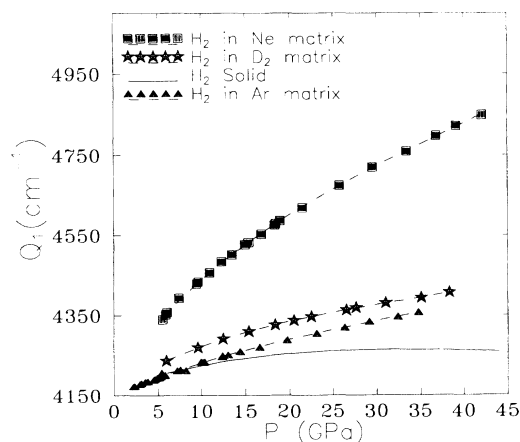


FIG. 6. Change vs pressure at room temperature of the Raman frequency of the $Q_1(1)$ vibron mode of the H_2 molecule isolated in various matrices. The squares represent the measurements in the Ne matrix; the stars, the ones in the D_2 matrix, and the triangles, the ones in the Ar matrix. The solid line is the third-order polynomial fit to the measurements in pure solid H_2 and the dashed lines, the fits of the data in matrices. The coefficients of these fits are given in Table II.

TABLE II. Coefficients of the third-order polynomial, $Q_1(\text{cm}^{-1}) = a_0 + a_1P + a_2P^2 + a_3P^3$ with P in GPa, fits to the Raman measurements of the shift with pressure of the $Q_1(1)$ vibron frequency of the H_2 molecule isolated in various matrices: Ne, Ar, D_2 , and H_2 .

System	a_0	a_1	a_2	a_3
H_2 in Ne	4210.97	26.836 9	-0.444 5	0.004 01
H_2 in Ar	4153	9.42232	-0.1636	0.00179
H_2 in D_2	4173.46	12.3444	-0.2661	0.00268
H_2 in H_2	4169.49	7.21588	-0.1712	0.00123

sites. Also, depending on the difference in the strength between the H_2 -host interaction and the host matrix interaction, a distortion of the matrix around the impurity exists that can induce an overcompression, as in the Ne matrix, or an undercompression, as in the Ar matrix.

Contrary to the observation in solid H_2 , no sign of a turnover of the $Q_1(1)$ vibron frequency shift is seen for the H_2 molecule isolated in matrices, which is all the more interesting in the case of H_2 in the D_2 matrix. This will be thoroughly analyzed in the next section and the reason for such a difference in solid H_2 will be attributed to the existence of a strong negative vibrational coupling between H_2 molecules.

V. DISCUSSION

Apart from the above-mentioned theoretical works in the low-density fluid phase, most of the calculations have been done in the crystalline phase. There, the calculations are simplified by the translational symmetry of the lattice and also numerous experimental data at $P=0$ could have been compared to theory. Let us briefly recall the various contributions to the change of the energy levels of a molecule embedded in a matrix.¹

In the molecular approach, the H_2 -host interaction Hamiltonian can be expressed as a function of the internal and angular coordinates of the diatomic molecule and of the external, R_i , guest-host coordinates. The terms of this Hamiltonian, which only depend on one coordinate, describe the static interaction and the ones which depend on at least two coordinates describe the coupling between excitations, known as the dynamical shift. An important element of simplification here, in the case of H_2 molecules, is to recognize that the rotational, translational, and intramolecular vibrational degrees of freedom are only weakly coupled to one another.¹⁸ This is due to the fact that the rotational state of the H_2 molecule is very near a free rotor,¹⁹ even up to 40 GPa, and also that the vibrational frequency is much greater than the rotational or phonon ones. Knowing that, the measured changes with pressure of the $Q_1(1)$ vibron frequency in the rare-gas or isotopic H_2 matrices are the results of three contributions.

(1) The static shift, which is a measure of the crystal compression on the molecule. It results from the bond-distance dependence of the H_2 -host interaction and from the change of the intramolecular potential upon strong confinement.

(2) The dynamical shift which results from the vibration-phonon coupling. In an Einstein-type formula-

tion, it means that the intermolecular H_2 -host interaction has to be averaged on the center-of-mass motions of the H_2 molecule and of its neighbors.

(3) The vibrational coupling which results from the resonance transfer of vibrational energy between two neighbor H_2 molecules.

The present set of experimental data allow a quantitative investigation of the importance of these various terms at high pressure.

A. The static shift: A limitation of the molecular description at high pressure

To our knowledge, only one calculation¹⁸ has attempted to calculate quantitatively the vibrational and rotational energy shifts of an isotopic H_2 molecule trapped in a rare-gas matrix under pressure, namely, Ar. Central to this $T=0$ -K calculation was the use of an improved expression for the H_2 -Ar potential,²⁰ the choice of an Ar-Ar potential which leads to a very good agreement with the experimental x-ray-determined equation of state²¹ at least up to 40 GPa, relaxation of the crystal lattice up to 16 shells around the impurity, and the consideration of zero-point oscillations of the H_2 molecule and its Ar neighbor atoms. Good agreement was obtained with the $P=0$ measurements. The present experimental data offer an experimental reference for a high-pressure quantitative comparison. Still, for a meaningful comparison with the present $T=296$ -K measurements, the importance of thermal effects should be first quantified.

In Fig. 7, the measurements of the vibron frequency

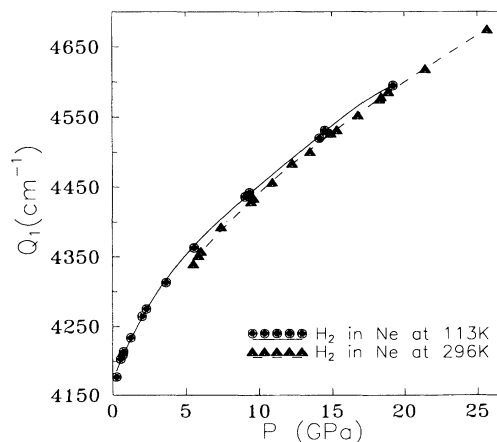


FIG. 7. Comparison between the change with pressure of the $Q_1(1)$ vibron frequency of the H_2 molecule isolated in the Ne matrix at 113 K, as circles, and at 296 K, as triangles. The lines are drawn as guide to the eyes.

shifts of H_2 in a Ne matrix are compared at 113 and 296 K. The difference is maximum near melting where it amounts to 11% of the shift but it then decreases with pressure to become negligible above 15 GPa. This difference is essentially due to the thermal expansion of the Ne lattice near melting which, at a given pressure, gives a smaller compression at 296 K than at 113 K. This comparison also indicates that the dynamical shift, which is certainly temperature dependent, should be quite small in matrices at high pressure, contrary to the situation¹⁸ at $P=0$. These conclusions can be straightforwardly extended to the Ar matrix. In Fig. 8, the H_2 vibron frequency shift measured in Ar at 296 K is compared to the above-mentioned $T=0$ K molecular calculation.¹⁸ The melting pressure of solid Ar at 296 K is 1.3 GPa. Knowing that differences due to thermal effect should only be important in the pressure domain above melting, the agreement between theory and experiment is thus satisfactory below 5 GPa. Above melting, however, the theoretical slope of the blue-shift variation is more than three times greater than the experimental one. This large discrepancy in the static shift could be attributed to an overestimate of the repulsive part of the H_2 -Ar interaction²⁰ but the error would then be unexpectedly large. More probably, what is in question here is the limit of the validity of the molecular approach, that is, when the density dependence of the intramolecular and intermolecular potentials has to be considered. As is well known from the heuristic box-model calculation,¹⁷ the intramolecular potential of the H_2 molecule changes with compression, mainly because of the increased kinetic energy of the electrons upon confinement. Also, the importance of many-body interactions in simple molecular systems under pressure has been demonstrated;²² they should also influence the molecule-matrix host interaction and they could be taken into account effectively averaged in the H_2 -host intermolecular pair potential which then would become density dependent. Instead, first-principles cal-

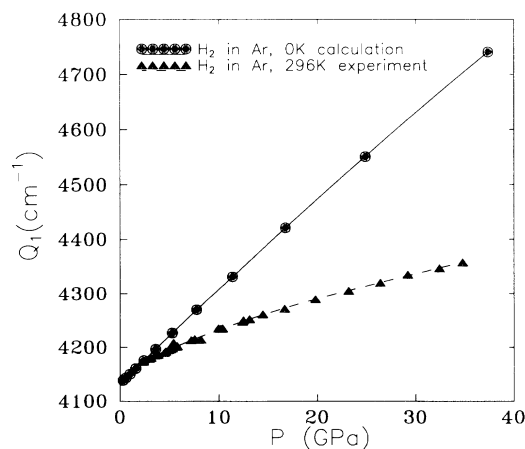


FIG. 8. Comparison between the experimental and the calculated changes with pressure of the Q_1 vibron frequency of the H_2 molecule isolated in an Ar matrix. The circles represent the $T=0$ K molecular calculation (Ref. 18) and the triangles, the $T=296$ K measurements.

culations starting at the electronic level would have to be performed in order to reproduce fully the present experimental data. In return, this comparison should constitute the most elementary test for state of the art *ab initio* calculations.

B. The vibrational coupling: Evidence for a charge-transfer interaction between H_2 molecules

The differences between the vibrational properties of the H_2 molecule isolated either in solid H_2 or in solid D_2 stem from the vibrational coupling contribution. At a given pressure, their static shifts should be exactly equal since, up to now, no significant isotope effect between the H_2 - H_2 or the D_2 - H_2 intermolecular potentials has been reported. Small differences might exist in their dynamical shifts, due essentially to the anharmonicity of the lattice mode but, as seen above, this dynamical contribution is relatively small under pressure.

The vibrational coupling between two H_2 molecules arises from the dependence of the H_2 - H_2 intermolecular interaction, here in the repulsive region, on the bond lengths of the two interacting H_2 molecules. The intermolecular potential between two quasifree rotor H_2 molecules can be written as $\Phi(R_{12}, r_1, r_2)$, where R_{12} is their intermolecular distance and r_1 and r_2 their bond lengths. Let us expand this interaction up to second order in the power of the variations, noted as u_1 and u_2 , of the bond lengths around their equilibrium values. Retaining non-vanishing terms and taking into account the fact that the equilibrium bond length, r_e , is a function of R_{12} , this gives

$$\Phi(R_{12}, r_1, r_2) = \Phi(R_{12}, r_e(R_{12}), r_e(R_{12})) + F(R_{12})(u_1^2 + u_2^2) + G(R_{12})u_1u_2. \quad (2)$$

The third term on the right-hand side of Eq. (2) is the one responsible for the vibrational coupling.

At a given pressure P , let us assume that ω_{un} would be the $Q_1(1)$ vibron frequency of the H_2 molecule in solid H_2 if the static and dynamical shifts were solely active. In a quasiharmonic formulation, we can write

$$\omega_{un} = \frac{1}{2\pi} \sqrt{F(P)/\mu}, \quad (3)$$

where $F(P)$ is an effective harmonic force constant and μ the reduced mass of the H_2 molecule. In this quasiharmonic approximation, at a given pressure P , the vibrational properties of solid H_2 can be modeled as the one of a hcp lattice of harmonic oscillators, $F(P)u_i^2/2$, coupled through the interaction $G(R_{ij})u_iu_j$. For the sake of simplicity, only the nearest-neighbor coupling is considered. The dynamical matrix of this system is straightforwardly calculated; its diagonalization for normal modes gives the vibrational energy band. The two solutions for $K=0$, corresponding to an even and odd interchange of the two sites of the hcp lattice, are particularly simple.

(1) The even $K=0$ mode, which is Raman active, has the following frequency:

$$\omega_{\text{Ram}} = \frac{1}{2\pi} \sqrt{[F(P) + 12G(R_1)]/\mu}, \quad (4)$$

R_1 being the nearest-neighbor distance at pressure P . For a small value of $G(R_1)$, Eq. (4) is equivalent to the result of the perturbational calculation, in terms of traveling vibrational excitations, of Van Kranendonk.^{15,23}

(2) The odd $K=0$ mode, which is infrared active, has a frequency equal to ω_{un} .

(3) For the H_2 molecule isolated in solid D_2 , there is no possibility of vibrational coupling due to mismatch of vibrational frequency between the guest and host molecules. In the quasiharmonic formulation, the H_2 vibron frequency should then be equal to ω_{un} .

The appropriateness of this analysis is illustrated in Fig. 9. The infrared measurement of the vibron frequency of H_2 in its solid²⁴ is very near the Raman measurements of H_2 in solid D_2 . They both differ from the Raman measurement of H_2 in its solid by the vibrational coupling contribution. The small difference between the infrared measurements of H_2 in its solid and the Raman measurements of H_2 isolated in solid D_2 can even be understood. Following Van Kranendonk,²³ the H_2 molecule is infrared active through an induced dipole mechanism; this breaks the $\Delta K=0$ selection rule and the infrared profile is then peaked at a frequency slightly shifted from the $K=0$ odd mode. The sign of this shift should be opposite to the one of the vibrational coupling, as observed in Fig. 9.

In the framework of the above quasiharmonic simple model, we can extract from our measurements of the vibron frequency of H_2 embedded in solid H_2 and in solid D_2 the nearest-neighbor vibrational coupling constant, $G(R_1)$, as a function of the intermolecular distance, R_1 , estimated from the experimental x-ray-determined equation of state.²⁵

The negative of the vibrational force constant $-G(R_1)$

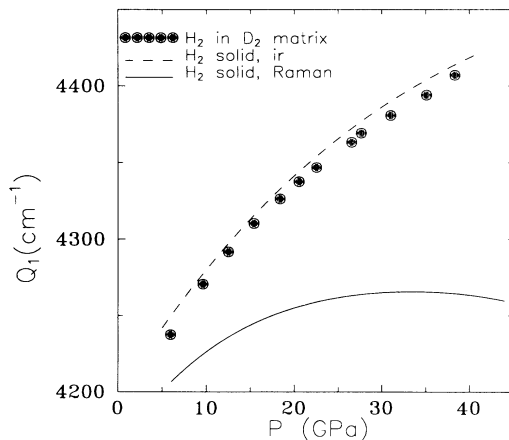


FIG. 9. Comparison between different room-temperature measurements of the $Q_1(1)$ vibron frequency change with pressure of the H_2 molecule embedded in isotopic H_2 solids. The circles indicate the Raman measurements of the H_2 molecule isolated in a D_2 matrix; the dashed line is the fit of the infrared measurements in solid H_2 (Ref. 24); the solid line is the third-order polynomial fit of the Raman measurement in solid H_2 .

is plotted as squares in Fig. 10. The star indicates the measurement in the low-pressure solid H_2 .¹⁶ The vibrational coupling was attributed there to the dipole-dipole interaction and was shown to change as $1/R_1^6$ at low density. The dashed line is the $1/R_1^6$ evolution extrapolated in the domain of intermolecular distances covered by the present experimental data. Around 2.4 Å, the measured coupling constant is already a factor of 2 greater than the extrapolated $1/R_1^6$ one. This difference is certainly too big so that it can be attributed to the flaws of our model, namely; the limitation of the vibrational coupling to nearest neighbors only, the quasiharmonic approximation, or the change of the constant of the $1/R_1^6$ coupling.

No *ab initio* calculation of the complete surface potential $\Phi(R_{12}, r_1, r_2)$ is available in the literature from which $G(R_1)$ could be calculated. Although Ree and Bender have considered bond-length variations in their *ab initio* calculation, unfortunately, they restrict it to the case of equal bond lengths of the two interacting molecules.²⁶

Such a negative vibrational coupling constant has been previously considered by Kobashi and Etters²⁷ as an *ad hoc* hypothesis in order to reproduce the vibron modes of dense solid I_2 and it was conjectured to result from an increasing charge-transfer interaction in the approach of metallization. The well-known phenomenon of tunneling allows the electron from one molecule to get into the region of a nearest-neighbor molecule. Such a charge-transfer configuration, in which there are net charges at each of the molecules, leads to an attractive covalent bonding component. The present work would then be a strong indication of the importance of such configurations, even between H_2 molecules separated by distances near the van der Waals minimum. This was

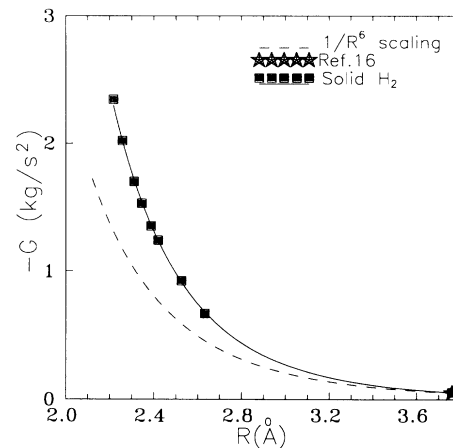


FIG. 10. The negative of the vibrational coupling constant, $-G$, as a function of the intermolecular distance, R , between nearest-neighbor H_2 molecules in their solid. The squares represent the data inverted from the Raman measurements of the vibron frequency shift of the H_2 molecule isolated in isotopic H_2 solids, as explained in Sec. V. The solid line is the best fit to these data, given by $G = -647/R^7$. The star is the low-pressure determination (Ref. 16) and the dashed line is the $1/R^6$ evolution expected from a dipole-dipole coupling mechanism (Ref. 16).

previously suggested by the *ab initio* calculation of Gallup.²⁸ Although neutral electronic configurations give the largely dominant repulsive contribution to the pair potential, the charge-transfer contribution could be dominant for vibrational coupling if it were much more dependent on the bond-length variations of the two nearest-neighbor interacting H₂ molecules.

Following Eters and Kobashi, the charge-transfer interaction should also give a positive contribution to the frequency of the E_{2g} optical phonon of the hcp solid H₂. This could help to thus resolve the discrepancy between experiment and the phonon calculations from effective pair potential fits to equation-of-state data which are systematically too low.²⁹

VI. CONCLUSION

The present work reports DAC measurements on the properties of H₂ molecules isolated in matrices at pressures above 1 GPa. The change with pressure of the vibron frequency of the H₂ molecule was investigated by Raman spectroscopy. This is certainly the easiest experiment to be performed, and interesting results have already been obtained.

(1) The vibron frequency shift up to 5 GPa provides valuable experimental information on the repulsive part of the H₂-rare-gas (He, Ne, or Ar) intermolecular potentials. Theoretical works are now needed to exploit them.

(2) Above approximately 5 GPa, it is shown that the molecular approach is not satisfactory. This is probably due to the change upon compression of the intramolecular potential of the H₂ molecule and to the growing importance of many-body intermolecular forces.

(3) The data on the H₂ molecule isolated in high-pressure solid Ne represent the best experimental analogue of this cornerstone system of physical chemistry: a compressed molecule in a box of shrinking volume. State of the art calculations of this problem should now be performed for comparison with the Ne experiment.

(4) The analysis of the measurements of the H₂ molecule isolated in a D₂ matrix has produced an understanding of the surprising turnover of the $Q_1(1)$ vibron fre-

quency shift of H₂ in its own solid around 30 GPa. This interesting feature is due to the unexpectedly large contribution of the resonance transfer of vibrational energy between H₂ molecules. The associated large negative vibrational constant, at intermolecular distances corresponding to the repulsive overlap region of the H₂-H₂ pair potential, could be a strong indication of the growing importance of charge transfer in solid H₂ in this density range. Further works are needed to settle this statement more firmly and to propose a charge-transfer potential with which the properties of molecular H₂ in condensed matter could be reproduced with standard statistical methods.

Recently, very high-pressure DAC experiments up to 250 GPa have been devoted to elucidate the picture of the transition to the metallic state of a dense system of H₂ molecules.^{29,30} The present article shows that two other systems deserve the same interest if a complete understanding of the gradual perturbation of the electronic properties of H₂ molecules under strong compression is to be reached: first, H₂ molecules isolated in a Ne matrix to probe a maximum static shift; second, H₂ molecules isolated in a D₂ matrix to probe the transfer of vibrational energy which could be related to a measure of the charge transfer. Work along these directions is in progress in our laboratory.

Finally, in the course of the present experiments, interesting results were obtained on the clustering of H₂ molecules in dense rare-gas matrices. They are planned to be reported in the future.

ACKNOWLEDGMENTS

We thank M. Jean-Louis for help with the experiments and helpful discussions and J. M. Besson for continuous interest in this work. We are grateful to W. B. Daniels for convincing us that the intermolecular vibrational exchange should be very important in dense solid H₂. This work was supported by the Commissariat à l'Énergie Atomique under Grant No. DAM/CEL-2561/3272. The Physique des Milieux Condensés is Unité Associée No. 782 du Centre National de la Recherche Scientifique.

¹H. Dubost, in *Inert Gases*, edited by M. L. Klein (Springer-Verlag, Berlin, 1984), pp.145–257.

²H. J. Jodl and K. D. Bier, in *Simple Molecular Systems at Very High Density*, edited by A. Polian, P. Loubeyre, and N. Boccaro (Plenum, New York, 1989), pp. 85–108.

³P. Loubeyre, R. LeToullec, and J. P. Pinceaux, *Phys. Rev. Lett.* **67**, 3271 (1991).

⁴S. K. Sharma, H. K. Mao, and P. M. Bell, *Phys. Rev. Lett.* **44**, 886 (1980).

⁵H. Vu, in *Matrix Isolation Spectroscopy*, edited by A. J. Barnes (Reidel, Dordrecht, 1980), Chap. 11.

⁶H. K. Mao, in *Simple Molecular Systems at Very High Density* (Ref. 2), pp. 221–236.

⁷R. LeToullec, J. P. Pinceaux, and P. Loubeyre, *High Pressure Res.* **1**, 77 (1988).

⁸H. K. Mao, J. Xu, and P. M. Bell, *J. Geophys. Res.* **91**, 4673 (1986).

⁹P. Dion and A. D. May, *Can. J. Phys.* **51**, 36 (1973).

¹⁰P. Loubeyre, R. LeToullec, and J. P. Pinceaux, *Phys. Rev. B* **32**, 7611 (1985).

¹¹F. Marsault-Herail, M. Echargui, G. Levi, and J. P. Marsault, *J. Chem. Phys.* **77**, 2715 (1982).

¹²D. Robert, J. Bonamy, J. P. Sala, G. Levi, and F. Marsault-Herail, *J. Phys. Chem.* **99**, 303 (1985).

¹³F. H. Ree, in *Simple Molecular Systems at Very High Density* (Ref. 2), pp. 153–180.

¹⁴V. Soots, E. J. Allin, and A. L. Welsh, *Can. J. Phys.* **43**, 1985 (1965).

¹⁵J. Van Kranendonk, *Physica* **25**, 1080 (1959).

¹⁶E. J. Allin and S. M. Till, *Can. J. Phys.* **57**, 442 (1979).

¹⁷R. LeSar and D. R. Herschbach, *J. Phys. Chem.* **85**, 2798 (1981).

¹⁸B. Silvi, V. Chandrasekharan, M. Chergui, and R. D. Eters, *Phys. Rev. B* **33**, 2749 (1986).

- ¹⁹P. Loubeyre, M. Jean-Louis, and I. F. Silvera, *Phys. Rev. B* **43**, 10 191 (1991).
- ²⁰R. Le Roy and J. Carley, *Advances in Chemical Physics*, edited by K. P. Lawley (Wiley, New York, 1980), p. 353.
- ²¹M. Ross, H. K. Mao, P. M. Bell, and J. Xu, *J. Chem. Phys.* **85**, 1028 (1986).
- ²²P. Loubeyre, *Phys. Rev. B* **37**, 5432 (1988).
- ²³J. Van Kranendonk, *Solid Hydrogen* (Plenum, New York, 1983).
- ²⁴H. K. Mao, J. Xu, and P. M. Bell, *Carnegie Institution Yearbook* (Carnegie, Pittsburgh, 1982), p. 366.
- ²⁵R. J. Hemley, H. K. Mao, L. W. Finger, A. P. Jephcoat, R. M. Hazen, and C. S. Zha, *Phys. Rev. B* **42**, 6458 (1990).
- ²⁶F. H. Ree and C. F. Bender, *J. Chem. Phys.* **71**, 5362 (1979).
- ²⁷K. Kobashi and R. D. Etters, *J. Chem. Phys.* **79**, 3018 (1983).
- ²⁸G. A. Gallup, *J. Chem. Phys.* **66**, 2252 (1977).
- ²⁹R. J. Hemley, H. K. Mao, and M. Hanfland, in *Molecular Systems Under Very High Pressure*, edited by R. Pucci and G. Piccitto (North-Holland, Amsterdam, 1991), pp. 223–244.
- ³⁰I. F. Silvera, J. H. Eggert, K. A. Goettel, and H. E. Lorenzana, in *Molecular Systems Under Very High Pressure* (Ref. 29), pp. 181–200.